# Application of Digital Phase Analysis to Far-Infrared Laser Interferometer for the Large Helical Device

Hikona SAKAI<sup>1</sup>), Kenji TANAKA<sup>1,2</sup>), Yuki TAKEMURA<sup>2,3</sup>), Yasuhiko ITO<sup>2</sup>), Tokihiko TOKUZAWA<sup>2,3</sup>), Ryo YASUHARA<sup>2,3</sup>), Hiyori UEHARA<sup>2,3</sup>), Toshiki KINOSHITA<sup>1</sup>), Tsuyoshi AKIYAMA<sup>2,a</sup>), Kazuya NAKAYAMA<sup>4</sup>) and Kazuo KAWAHATA<sup>2</sup>)

<sup>1)</sup>Interdisciplinary Graduate School of Engineering Sciences, Kyushu University, Kasuga, Fukuoka 816-8580, Japan <sup>2)</sup>National Institute for Fusion Science, Toki, Gifu 509-5292, Japan

<sup>3)</sup>The Graduate University for Advanced Studies, SOKENDAI, Toki, Gifu 509-5292, Japan

<sup>4)</sup>College of Engineering, Chubu University, Kasugai, Aichi 487-8501, Japan

(Received 31 August 2022 / Accepted 22 May 2023)

A digital phase analysis technique was applied to a 119-µm wavelength far-infrared (FIR) laser interferometer on the Large Helical Device (LHD). High-density plasma measurement without phase jumping was achieved, representing an improvement over measurements made using a conventional analog phase counter. Digital phase analysis became operational at a quarter of the threshold of the analog phase counter. The phase sensitivity was also improved using digital analysis because the noise level was reduced to approximately half that of the conventional analog phase counter. The improved phase sensitivity enabled measurement of small-amplitude fluctuations.

© 2023 The Japan Society of Plasma Science and Nuclear Fusion Research

Keywords: plasma, interferometer, far-infrared laser, digital demodulation

DOI: 10.1585/pfr.18.1402062

## 1. Introduction

Interferometers are widely used to measure the electron density in high-temperature plasma. When the frequency of the incident laser is considerably higher than the cut-off frequency, phase differences of the laser, caused by variations in the electron density are determined only by the laser wavelength and the line integral of the electron density along the beam axis. One of the advantages of the interferometers is high measurement accuracy [1–3]. For heterodyne detection, interference phase shifts are not affected by changes in the laser power and detector sensitivity, so absolute calibration is not necessary. In contrast, the absolute calibration is required for electron density measurement by Thomson scattering.

An interferometer is indispensable in plasma experiments for monitoring the electron density and as a source of feedback signals for density control. However, an interferometer sometimes fails during measurement because of the occurrence of "phase jump," which is problematic for physical analysis and real-time density monitoring. Phase jumps frequently in the presence of steep density gradients, such as those generated during pellet injection and radiation collapse. Phase jumps can be prevented using other diagnostic instruments, such as the Faraday rotation polarimeter [4, 5], the Cotton-Muton ellipticity polarimeter [6], and the dispersion interferometer [7]. These instruments have application potential in future reactors for highdensity operations. However, these instruments are technically difficult because a smaller phase shift occurs than an interferometer. As interferometers are mainly used to measure the electron density in most current working devices, improvements in phase detection are essential. An interferometer can also be used to measure macro- and microscale instabilities, the amplitude of which is less than 10% of the background density. Thus, it is also important to increase the phase resolution.

In this study, we used digital phase analysis to improve phase measurement. This technique was applied to a 119  $\mu$ m-wavelength far-infrared (FIR) laser interferometer currently working on the Large Helical Device (LHD) [8–10]. The technique improved to prevent phase jumping and enabled to measure small variations in phases. Consequently, magneto-hydro dynamics (MHD) fluctuations driven by fast ions could be clearly measured.

In Sec. 2, an overview of the FIR laser interferometer for LHD is presented, and conventional analog phase detection and the digital phase analysis technique are described. In Sec. 3, an example is presented to demonstrate the prevention of phase jumping and improved measurements of small variation in phases. Finally, a discussion and summary are presented in Sec. 4.

author's e-mail: h.sakai@triam.kyushu-u.ac.jp

<sup>&</sup>lt;sup>a)</sup> Present address: General Atomics, P. O. Box 85068, San Diego, CA 92186-9784, USA

# 2. FIR Laser Interferometer System for LHD

## 2.1 Overview of the interferometer system

Figure 1 (a) shows a cross-sectional view of LHD and the FIR laser system [10]. The optical system is configured as a heterodyne Michelson interferometer. The probe beam is split into 14 chords, of which 13 are plasma probe beams and one is a reference probe beam. The plasma probe beams and the reference probe one pass through a vacuum vessel, and then mix with the local beam in the interferometer housing, producing plasma beat and reference beat signals, whose frequencies are defined as  $\omega_{IF}$ . The cavity length of the laser is controlled to maintain the beat frequency of 1 MHz. Schottky barrier diodes (SBDs) are used for detection [8, 10]. As an SBD has a maximum frequency response of approximately 2 MHz,  $\omega_{IF}/2\pi$  is set at 1 MHz. The plasma beat and reference beat signals are sent to an analog phase counter and a digital phase analysis system.

A schematic of the signal processing is shown in Fig. 1 (b). In the conventional method, the plasma beat and reference beat signals are input to an analog phase counter [11], and the output of the phase counter is acquired by an analog digital converter (ADC). In the novel digital phase analysis, plasma beat and reference beat sig-

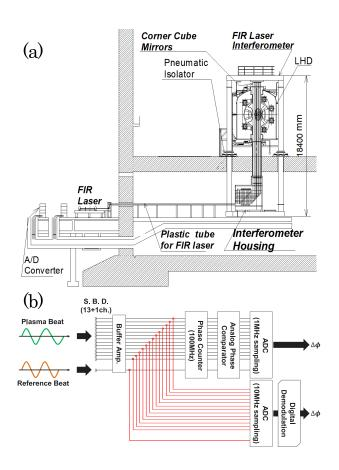


Fig. 1 (a) LHD cross-section and overview of the FIR laser interferometer system, (b) Schematic of a signal processing system.

nals are directly acquired by the ADC, and the phase shifts are evaluated using a numerical technique that will be described later.

### 2.2 Phase counting technique

There are several schemes for using an electrical circuit to perform phase counting. One typical technique involves the use of a quadrature phase counter. The heterodyne beat signal with  $\omega_{IF}$  is converted to sine and cosine signals, which are known as quadrature or I/Q signals. The ratio of the sine and cosine signals provides phase information about the phase. The measured phase folds back every  $\pi$  rad. It is inconvenient to estimate the continuous phase shift larger than  $\pi$  rad. The analog phase counter developed for the FIR laser interferometer for LHD can continuously measure phase shifts larger than  $\pi$  rad without phase resetting [11, 12].

Now, the reference signal is denoted as  $\cos(\omega_{IF}t)$ , and the probe signal is denoted as  $\cos(\omega_{IF}t - \Delta\phi)$ , where  $\Delta\phi$ is the phase shift caused by a change in the line-averaged electron density. A field-programmable gate array (FPGA) in the analog phase counting system evaluates the phase shift  $\Delta\phi$  between the plasma beat and reference beat signals by measuring the time at which the signal exceeds a threshold voltage of 100 mV. The finite threshold is set to prevent phase counting caused by noise. The FPGA measures the delay time  $\Delta t$  and the phase shift is evaluated as  $\Delta\phi = \omega_{IF} \times \Delta t$ . When  $\Delta\phi$  exceeds  $2\pi$ , the number of  $2\pi$  phase shifts (the number of interference fringes) is counted, and the remaining phase shifts are summed.

It is essential to use an analog phase counter in experiments to enable real-time output. Thus, an analog phase counter can be used to realize real-time density monitoring and as a signal source for density feedback control. However, three technical problems are associated with the use of an analog phase counter.

First, in this scheme, when the phase changes  $2\pi$  during one reference time period (1 µsec), the phase shift cannot be evaluated. However, a phase shift this large, which corresponds to a change in the electron density of  $0.5 \times 10^{19}$  m<sup>-3</sup> over 1 µsec, is highly unlikely and does not occur even during pellet injection or radiation collapse.

Second, when the plasma beat signal amplitude decreases below the threshold voltage, time-delay counting is not operational. This is called phase jump. The decrease in the signal amplitude is caused by refraction. A steep density gradient appears in the case of pellet injection or radiation collapse.

Third, the phase resolution is limited to  $2\pi/100$  because a 100-MHz clock counter is used for a 1-µsec time period. This phase resolution is sufficient to measure electron density but not small-amplitude fluctuations. In the next subsection, we describe how digital phase demodulation can mitigate the second and third problems.

#### 2.3 Digital phase counting system

To overcome the aforementioned problems, digital phase counting was employed to perform digital phase analysis. The digital phase counting technique was first reported in Ref. [13]. This method consists of applying numerical analysis techniques (a Hilbert transform and a phase calculation using complex functions) to digitally sampled plasma beat and reference beat signals. The beat signal is expressed as follows:

$$x(t) = A(t)\cos\{\omega_{IF}t + \phi(t)\},\tag{1}$$

where A(t) is the amplitude of the plasma beat signal.

The Hilbert transform of Eq. (1) is expressed as

$$x'(t') = A(t')e^{-i\{\omega_{IF}t' + \phi(t')\}},$$
(2)

Equation (2) can be expressed using Euler's formula as

$$x'(t') = A(t')[\cos\{\omega_{IF}t' + \phi(t')\} - i\sin\{\omega_{IF}t' + \phi(t')\}].$$
(3)

Examination of Eqs. (1) and (3) shows that Eq. (3) contains a component with a phase shifted by  $90^{\circ}$  from the original real signal. Equation (3) can be used to derive the instantaneous values of the amplitude and phase as follows:

$$A(t') = \sqrt{x'(t')^2},$$
 (4)

$$\phi(t') = \operatorname{atan} \frac{\operatorname{Im}\{x'(t')\}}{\operatorname{Re}\{x'(t')\}}.$$
(5)

The procedure presented above can be applied to the plasma beat and reference beat signals, and the phase difference between these signals can be calculated to yield the time evolution of the phase change induced by the plasma.

The aforementioned procedure can also be effectively applied to discrete data, which is known as digital demodulation. The phase variation can be calculated for each sampling period. Then, the phase can be estimated temporally and continuously. In addition to phase determination, a phase reset of  $\pi$  rad takes place every  $\pi$  phase shift. This phase reset can be easily corrected numerically.

# 3. Comparison between Analog Phase Counting and Digital Phase Demodulation

In the following two sub-sections, the techniques of analog phase counting and digital phase demodulation are compared in terms of the mitigation of phase jumps during pellet injection discharge and improvements in the phase resolution for fluctuation measurements.

### 3.1 Mitigation of the phase jump during pellet injection discharge

The pellet injection is a powerful technique for fueling and investigation of particle transport. In LHD, hydrogen and deuterium ice pellets are injected for core fueling [14]. The analog phase counter system that is frequently used with the FIR laser interferometer to measure the electron density after the pellet injection sometimes fails because of phase jumping.

Figure 2 shows the temporal evolution of the lineaveraged density and beat signal amplitude. Figure 2 (a) shows the electron density measured using an analog phase counter and digital phase demodulation. Figure 2 (b) shows the temporal evolution of the amplitude of the plasma beat and reference beat signals.

Digital demodulation consisted of acquiring beat signals 10-MHz sampling and applying the analysis techniques described in Sec. 2.3. The analog and digital signal processes were performed using the same interferometer channel.

Figure 2 (a) shows that a phase jump occurred at t = 3.71 sec in the analog phase counter when the amplitude of the plasma beat signal decreased to below the threshold voltage for phase counting (shown in Fig. 2 (b)). Refraction reduced the plasma probe beam intensity, which in turn reduced the beat signal amplitude. The minimum amplitude of the plasma beat signal in Fig. 2 (b) is 0.0233 V. This value was approximately a quarter of the threshold voltage of the analog phase counter, which subsequently failed to work.

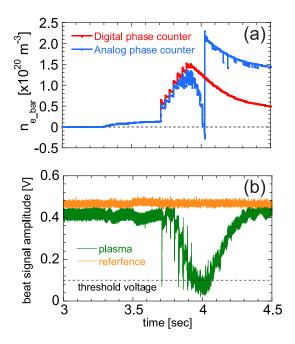


Fig. 2 Comparison of the results obtained using an analog phase counter and digital phase demodulation. The time history of (a) the line-averaged electron density and (b) the amplitudes of the plasma beat and reference beat signals. Eight pellets were injected. LHD shot #166573. The line-averaged density was defined as the line integral of the density close to magnetic axis normalized by the path length of the last closed flux surface in a vacuum magnetic configuration. The path length was 1.86 m.

The ablation process for hydrogen and deuterium pellets typically takes from 30 - 300 µsec. Figure 2 (a) shows an increase in the line-averaged density at t = 3.7 sec of the first pellet injection of approximately  $7 \times 10^{19}$  m<sup>-3</sup>, corresponding to a phase shift of 42 rad. The subsequent frequency shift was approximately 20 - 200 kHz. If a frequency shift exceeds 1 MHz, the analog phase counter does not follow the phase shift. However, this behavior is not observed in Fig. 2. Therefore, the phase jump of the analog phase counter was not caused by the rapid increase in density but by the decrease in the beat signal amplitude.

In contrast, digital phase demodulation effectively followed the change in the electron density after the pellet injection. The phase was correctly evaluated as long as the beat signal maintained a sinusoidal shape. The digital demodulation technique decreased the noise level more effectively than the analog phase counter.

## 3.2 Improvement of fluctuation measurement capability

In addition to removing phase jumps, the digital demodulation technique improved the measurement resolution, enabling the measurement of MHD fluctuations. In an analog phase counter system, 100-MHz clock counting limits the phase resolution to  $2\pi/100$ . This limitation does not exist for digital phase demodulation.

We compared the phase resolution of the analog and digital techniques for the measuring fast-ion driven instability. Figure 3 shows the time evolution of neutral beam injection (NBI) heating plasma. The intermittent signal of the magnetic probe shown in Fig. 3 (b) is an indication of a fast-ion driven instability [15]. When the NBI power was stepped down, the spectral peak of the intermittent signal changed. These results indicate that the fast-ion energy distribution affected the instability.

Electron density fluctuations were simultaneously measured using the analog phase counter and digital phase demodulation, and the results are shown in Figs. 3 (c) and (d), respectively. The change in the frequency spectrum was clearly measured by digital phase analysis (as shown in (d)) but not by the analog phase counter (as shown in (c)). During the high NBI power period, which lasted up to 4.4 sec, intermittent fluctuations appeared at approximately 25 kHz and the frequency shifted with each stepdown of the NBI power and disappeared at 4.55 sec. This result was explained in term of the step-down of the NBI power, which reduced the density of fast ions and consequently stabilized the fast-ion excitation mode.

Figure 4 shows the frequency spectrum during the period over which intermittent fluctuations were observed. The red and blue solid lines represent the electron density fluctuation spectra obtained with plasma using the analog phase counter and digital phase demodulation, respectively. Orange and light blue dashed lines represent the spectra obtained without plasma, respectively.

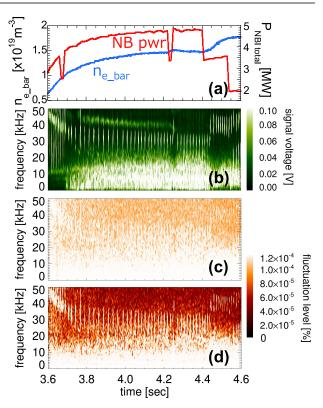


Fig. 3 Time evolution of (a) the NBI power (red) and lineaveraged density (blue); (b) the magnetic fluctuation spectrum of the magnetic probe; and the density fluctuation spectrum obtained using (c) the analog phase counter and (d) digital phase demodulation. LHD shot #162539.

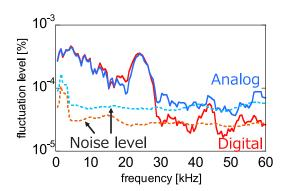


Fig. 4 Frequency spectrum during intermittent fluctuations.

Both the conventional and proposed methods enabled the observation of large-amplitude fluctuations at approximately 25 kHz. However, small amplitude fluctuations at approximately 43 kHz could only be measured using the digital technique because the noise level was approximately half that of the analog technique. Thus, clear fluctuation peaks appeared in the spectrum obtained using the digital technique.

# 4. Conclusion

A digital phase demodulation system was installed for the first time in an FIR laser interferometer system for LHD. A 10-MHz sampling process was used to directly acquire 1-MHz plasma beat and reference beat signals. Compared with a conventional phase counter system, phase jumping after pellet injection was mitigated when the signal voltage dropped to a quarter of the threshold of the analog phase counter. The phase resolutions were also improved because the noise level of the digital system was half that of the conventional system. The digital phase demodulation technique became operational when the amplitude of the beat signal decreased below the threshold of the analog phase counter.

The enhancement of the phase resolution and reduction of the noise level enabled detailed elucidation of the spectrum of the fast-ion-driven MHD instability. As 10 -11 channels in the plasma were available, the integratedfluctuation signal provided essential information about the spatial structure of the MHD mode. The results were compared with theoretical model [15].

The proposed method has several limitations. Currently, the implementation of the digital phase demodulation technique requires enormous quantities of data for the 10-MHz sampling. The considerable time required for analysis precludes outputting in real-time. The application of the FPGA to digital demodulation will enable real-time operation [16]. The proposed digital technique does not completely remove the phase jump. The digital technique is not for signal amplitudes close to zero. In this case, a short-wavelength laser (e.g., a CO<sub>2</sub> laser with a wavelength of 10.6  $\mu$ m), which has low refraction can be used [17, 18].

# Acknowledgments

The authors express their deepest gratitude to the late Professor Shigeki Okajima of Chubu University for

his outstanding contribution to the development of the far-infrared laser interferometer for LHD. The authors would also like to thank Professor Ryuichi Sakamoto of the National Institute for Fusion Science for a fruitful discussion about the pellet ablation process. The authors would like to thank the LHD experimental group for excellent operation of LHD. LHD data can be accessed from the LHD data repository at https://wwwlhd.nifs.ac.jp/pub/Repository\_en.html. This study was supported by the NIFS grant NIFS20ULHH004 and NIFS21ULHH004, Junichi Miyamoto Hydrogen Research Award, and NIFS Research Fellows program.

- The Japan Society of Plasma Science and Nuclear Fusion Research, *Principles and Applications of Plasma Diagnostics*, (Corona Publishing Co., Ltd., 2006) (in Japanese).
- [2] L.H. Hutchinson, *Principle of Plasma Diagnostics*, Second edition (Cambridge University press, 2005).
- [3] D. Véron, *Infrared and Millimeter Waves*, Vol.2 (Academic Press, 1979).
- [4] K. Tanaka et al., Rev. Sci. Instrum. 70, 730 (1999).
- [5] T. Akiyama *et al.*, Rev. Sci. Instrum. **74**, 112 (2003).
- [6] T. Akiyama et al., Rev. Sci. Instrum. 77, 10F118 (2006).
- [7] T. Akiyama et al., JINST 15, 101004 (2020).
- [8] K. Kawahata et al., Fusion Eng. Des. 34-35, 393 (1997).
- [9] K. Tanaka *et al.*, Plasma Fusion Res. **3**, 050 (2008).
- [10] T. Akiyama et al., Fusion Sci. Technol. 58, 352 (2010).
- [11] Y. Ito et al., Fusion Eng. Des. 56-57, 965 (2001).
- [12] T. Tokuzawa et al., Rev. Sci. Instrum. 72, 1103 (2001).
- [13] Y. Jiang et al., Rev. Sci. Instrum. 68, 902 (1997).
- [14] R. Sakamoto et al., Rev. Sci. Instrum. 84, 083504 (2013).
- [15] K. Ogawa et al., Nucl. Fusion 62, 112001 (2022).
- [16] Y. Yao et al., Rev. Sci. Instrum. 93, 034705 (2022).
- [17] K. Tanaka et al., Plasma Fusion Res. 2, S1033 (2007).
- [18] Kinoshita et al., Plasma Fusion Res. 17, 1402107 (2022).